# Northumbria University

## Department of Mechanical and Construction Engineering

## Faculty of Engineering and Environment

## SIMULATION OF DUAL-FUEL DIESEL COMBUSTION WITH MULTI-ZONE FUEL SPRAY COMBUSTION MODEL

**Andrey Kuleshov**
Northumbria University
Newcastle upon Tyne, UK

**Khamid Mahkamov**
Northumbria University
Newcastle upon Tyne, UK

**Andrey Kozlov**
NAMI, Moscow, Russia

**Yury Fadeev**
Bauman Moscow State Technical University,
Moscow, Russia

<div align="center">

# DRAFT

</div>

# ICEF2014-5700

## SIMULATION OF DUAL-FUEL DIESEL COMBUSTION WITH MULTI-ZONE FUEL SPRAY COMBUSTION MODEL

**Andrey Kuleshov**
Northumbria University
Newcastle upon Tyne, UK

**Khamid Mahkamov**
Northumbria University
Newcastle upon Tyne, UK

**Andrey Kozlov**
NAMI, Moscow, Russia

**Yury Fadeev**
Bauman Moscow State Technical University,
Moscow, Russia

## ABSTRACT

There is increasing interest in application of various alternative fuels in marine diesel engines, including methanol. One of the challenges in the relevant research is the development of computer codes for simulation of the dual-fuel working process and engineering optimization of engines. In this work the mathematical model is described which simulates a mixture formation and combustion in an engine with a dual-fuel system, in which methanol is used as main fuel and a pilot portion of diesel oil is injected to ignite methanol. The developed combustion model was incorporated into the existing engine full cycle thermodynamic simulation tool, namely DIESEL-RK [1]. The developed combustion model includes the self-ignition delay calculation sub-model based on the detail chemistry simulation of methanol pre-combustion reactions, sub-model of evaporation of methanol droplets, sub-models of methanol fuel sprays penetration, spray angle and droplets forming, respectively. The developed computer code allows engineers to account for the arbitrary shape of the combustion chamber. Additionally, each fuel system (for methanol and diesel oil) may include several injectors with arbitrary oriented nozzles with different diameters and central, off-central and side location in the combustion chamber. The fuel sprays evolution model consists of equations with dimensionless parameters to account for fuel properties and in-cylinder conditions. Specifics of injection pressure profiles and interaction of sprays with the air swirl and between themselves are also considered. The model allows engineers to carry out rapid parametric analysis. Results of modelling for a medium speed dual-fuel diesel engine are presented which demonstrate a good agreement between calculated and experimental heat release curves and integral engine data.

## INTRODUCTION

Compression Ignition Engines running on alternative fuels have been the subject of special attention for several decades. One of the major problems in these CI engines is controlling of the start of ignition of the air/fuel mixture. Application of dual-fuel systems is one of effective solutions for this problem. Usually, fuel with low self-ignition properties such as petrol, methanol, ethanol or natural/bio gas is port injected or injected into the cylinder. Another fuel with the high reactivity (such as diesel, biodiesel or dimethyl ether is injected into the cylinder and initiates the combustion process. Application of dual-fuel systems along with EGR and controllable turbo charging allows engineers to organize the working process over a wide range of operational conditions using various fuels, including the alternative ones. In doing so it is possible to achieve the high efficiency and ultra-low emissions at part- and full-load regimes of operation. For example, Kokjohn et al. [2] tested a single cylinder heavy-duty Caterpillar engine with the compression ratio of 16.1. For the IMEP value ranging from 4.6 bar to 14.6 bar, NOx and soot emissions below 0.1 g/kWh and

0.013 g/kWh, respectively, and a peak gross indicated efficiency of 56% were demonstrated.

Methanol is currently attracting growing attention as alternative fuel because it is produced in large quantities using various sustainable biomass stocks and its excellent combustion properties. Methanol has a good prospective in duel-fuel engines since its RON is 110 and it has a very high self-ignition temperature. Additionally, methanol has the very high heat of evaporation which results in reduction of the temperature of fresh air/fuel charge in the cylinder and leads to lower thermal stresses in engine components and reduced formation of NOx.

A dual-fuel engine running on methanol and diesel oil was investigated in [3]. The author of [13] reported that in experiments 90% of diesel oil was replaced by methanol with efficiencies obtained being very close to that of the conventional engine running on 100% diesel oil. He also claims that results demonstrated that NOx emissions were reduced by half and HC emissions were cut by factor of 2-5. Exhaust smoke and particulate matter emissions were considerably reduced to the level of the nearly smoke-free operation.

Modern common rail fuel systems provide much finer atomisation of the fuel and high precision control of the mass of fuel injected into the cylinder. Recent investigations of the duel-fuel engine in [4] demonstrated that 93% of diesel can be replaced by methanol. In these tests the engine's indicated efficiency was 51.3% with the level of NOx and PM emissions being at the level of 0.07 g/kWh and 0.01 g/kWh, respectively.

In order to take a full advantage of application of methanol as an alternative fuel, it is necessary to optimise the engine design parameters such as the geometry of the combustion chamber, location of fuel injectors and orientation of their nozzles, fuel injection timing, control of turbo charging and EGR. Currently, this type of optimisation is achieved either experimentally or using CFD modelling. The first method requires significant time and resources and the latter one is difficult for application in practical engineering projects on optimisation and controlling of the fuel injection system due to considerable computational time involved and problem with automatic generation of input data for CFD simulation.

In this study an attempt is made to develop a zero-dimensional mathematical model of the working process, which can be used for high accuracy simulations of engines with a dual-fuel system and for optimisation of the engine design and operational parameters. The engine with methanol/diesel dual-fuel system was investigated. The theoretical basis of this project is the multi-zone diesel spray combustion model described in [5, 6]. This model was successfully applied previously, demonstrating very good correlation between obtained theoretical and experimental results for engines with a single- and multi-stage fuel injection [7-10] and for application of biofuel [11, 12]. The theoretical background of splitting fuel sprays into 10 characteristic zones (see Fig. 1), calculation of evolution of the length and shape of the fuel sprays, their interaction with the air flow, walls and each other and also calculations of their evaporation and combustion are described in detail in [5-12]. The small number of zones in the calculation

scheme allows radically decrease computing time in comparison with CFD. This approach and procedures along with the capability of the model to simulate the combustion process with a multi-stage injection of fuel can be extended to modelling of dual-fuel engines by replacing diesel fuel by another type of fuel in one of phases/stages of injection.
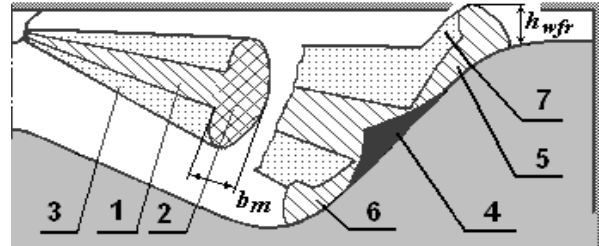


Figure 1. Characteristic zones of the fuel spray.
1 - Dense conical core of free spray; 2 - Dense forward front of free spray; 3 - Dilute outer sleeve of the free spray in which evaporation conditions are most favorable; 4 - Axial conical core of a NWF (fuel does not evaporate in this zone); 5 - Dense core of the NWF on a piston bowl surface; 6 - Dense forward front of the NWF; 7 - Dilute outer zone of NWF;

Mainly a diesel fuel spray is split in 7 characteristic zones, Fig. 1. In addition to zones, indicated in Fig. 1, three further zones can be formed during simulations: if the spay reaches the surface of the cylinder and/or head of the cylinder then zones 8 and 9, respectively, are formed. If there is overlapping between the NWF of individual spays then zone 10 will be formed in which the NWF of individual spays interact.

Equations which are used for calculation of the geometry of evolving spays and diameters of droplets of diesel fuel were derived by A.S. Lyshevsky [13]. These equations use dimensionless parameters defined by physical properties of fuel and environment in which the evolution of fuel sprays occurs. Modelling of dual-fuel engines is carried out with the assumption that those equations can also accurately describe the process of the spray evolution and combustion of alternative fuels if their properties are used for determination of the numerical values of the above dimensionless parameters. In this work the models previously used by authors in [5-12] were further developed to compute combustion when some of phases/stages of the fuel injection process are used to deliver alternative fuel, namely methanol, by means of the second independent fuel supply system. Since methanol has the greater enthalpy of evaporation and higher self-ignition temperature in comparison with diesel oil the following refinements were made in the basic mathematical model:

-The sub-model for calculation of evaporation of methanol droplets under in-cylinder conditions was developed;

-The sub-model for the rapid calculation of the process of self-ignition of methanol in the engine's cylinder was created;

-The sub-model of calculation of in-cylinder processes during the combustion phase was modified to take into account the high enthalpy of evaporation of methanol.

-The interface of DISEL-RK software for modelling of IC engines was modified in order to provide an opportunity to

specify input parameters to describe several independent fuel supply systems which could deliver different types of fuel into the cylinder.

Obtained results of simulation were then compared to available experimental data.

Though this study was focused on the combustion of methanol, the above modifications of the mathematical model and software were carried out in such way that to have a capacity to include into modelling process a wide range of fuels and their mixtures and different configurations of independent fuel supply systems.

## CALCULATION OF EVAPORATION OF INJECTED FUEL

Accurate calculation of the evaporation rate of fuel droplets during air-fuel mixing and combustion processes is of a paramount importance in modelling engines since the fuel evaporation rate determines the heat release dynamics during combustion [5, 6].

The rate of the change in the diameter of the fuel droplets prior and after ignition is defined using the equation by B.I. Sreznevskiy:

$$d_k^2 = d_0^2 - K\,\tau_u \qquad (1)$$

where $d_0$ and $d_k$ are the initial and current diameters of the droplet, respectively; $K$ is the evaporation constant, $\tau_u$ is the time elapsed from the instance when the droplet entered the corresponding characteristic zone. Modern fuel injection systems provide a high uniformity in atomisation of fuel and therefore calculations of the fuel droplets evaporation rate can be carried out using the value of the mean Sauter diameter of the droplet $d_{32}$. It is assumed in calculations that $d_0 = d_{32}$.

The mean Sauter droplet diameter $d_{32}$ is calculated using the dimensionless parameters [13] as follows:

$$d_{32} = 1.7\,d_n\,M^{0.0733}\left(\rho We\right)^{-0.266}, \qquad (2)$$

where $We = U_{0m}^2\,d_n\,\rho_f/\sigma_f$ , $\qquad (3)$

$$M = \mu_f^2 / \left(\rho_f\,d_n\,\sigma_f\right), \qquad (4)$$

$$\rho = \rho_{air}/\rho_f\ ; \qquad (5)$$

Here $d_n$ is the diameter of injector nozzles [m]; $We$ – Weber's number which is the ratio of the inertial force and surface tension; $M$ is the squared Ohnezorge number, the parameter defined by the ratio of forces due to the surface tension, inertia and viscosity; $\rho$ is the ratio of the air density $\rho_{air}$ in the cylinder and fuel density $\rho_f$, $U_{om}$ is the velocity of fuel in the nozzle exit [m/s], $\sigma_f$ is surface tension factor of fuel [N/m] and $\mu_f$ is the fuel dynamic viscosity coefficient [Pa s].

The evaporation constant $K_i$ is calculated for each characteristic zone $i$ as

$$K_i = 4\cdot10^6\,Nu_{Di}\,D_{pi}\,p_{Si}\,/\rho_f\ , \qquad (6)$$

Where: $Nu_{Di}$ is the Nusselt's number for the diffusion process in the individual zone [6]; $D_{pi}$ is the baro-diffusion coefficient for the individual zone:

$$D_{pi} = D_{po}\left(T_{ki}/T_o\right)\left(p_o/p\right)\,. \qquad (7)$$

The baro-diffusion coefficient $D_{pi}$ depends on the equilibrium temperature of the droplet $T_{ki}$ and current in-cylinder pressure $p$. In Eq. (6) $p_{Si}$ is the saturated vapor pressure at the temperature $T_{ki}$ for the individual zone; $D_{po}$ is the baro-diffusion factor determined for atmospheric conditions $[p_o, T_o]$.

The baro-diffusion factor $D_{po}$ is calculated as

$$D_{p0} = \frac{D_{c0}}{R_{vap}\,T_0}\ , \qquad (8)$$

where $D_{co}$ is the coefficient of concentration diffusion [m²/s]; $R_{vap}$ [J/(kg K)] is the specific gas constant for fuel vapour and $T_o = 273$ K.

$$R_{vap} = \frac{R}{\mu}, \qquad (9)$$

where $\mu$ is the molecular mass of fuel [kg/kmol], $R$ is the universal gas constant equal to 8310 J/(kmol K).

The vapour saturation pressure can be determined from Clausius-Clapeyron equation:

$$p_S = \exp\left(A - B/T_{ki}\right), \qquad (10)$$

where $T_{ki}$ is equilibrium temperature of the droplet.

Coefficients $A$ and $B$ in Eq. (10) are determined using two sets of known values of the saturated pressure and temperature:

$$B = \frac{\ln(p_{Scr}) - \ln(p_{S1})}{\dfrac{1}{T_1} - \dfrac{1}{T_{cr}}}; \qquad A = \ln(p_{S1}) + \frac{B}{T_1}. \qquad (11)$$

Here $p_{S1}$ is the saturated vapour pressure at some low temperature $T_1$ and $p_{Scr}$ is the saturated vapour pressure at the critical temperature $T_{cr}$.

The equilibrium temperature of the droplet $T_{ki}$ is determined using the equation of the energy balance between the heat delivered to the droplet from ambient air due to the heat conductivity and the heat consumed during heating of the liquid fuel, its evaporation and superheating of vapour to the temperature $T_{ki}$.

The fuel temperature in the centre of the droplet is assumed be equal to the surface temperature $T_{ki}$. The energy balance equation for this case is proposed by D.N. Vyrubov [14, 15]:

$$\lambda_a\left(T_i - T_{ki}\right) = D_{pi}\,p_{Si}\left[C_f\left(T_{ki} - T_f\right) + h_{evap} + C_{fv}\frac{T_i - T_{ki}}{2}\right], \quad (12)$$

where $T_i$ is the temperature in the characteristic zone [K]; $\lambda_\alpha$ is the coefficient of the heat conductivity in air for the current temperature and pressure in the cylinder [W/(m K)]; $C_f$ is the heat capacity of fuel [J/(kg K)]; $T_f$ is the initial temperature of fuel [K]; $h_{evap}$ is the enthalpy of evaporation of fuel [J/kg] and $C_{fv}$ is the heat capacity of fuel vapour [J/(kg K)]. In Eq. (12) the values of $p_{Si}$ and $\lambda_\alpha$ depend on $T_{ki}$.

Physical and chemical properties of diesel fuel and methanol used in calculations are presented in Table 2.

Fig. 2 shows results of calculation of the equilibrium temperature of droplet for diesel oil and methanol as a function

of the temperature in the dilute outer characteristic zone of the fuel spray.

Fig. 3 presents results of calculation of the duration of full evaporation of fuel droplets with diameter of 10 μm as a function of the temperature $T_i$ in the dilute outer characteristic zone of the fuel spray. For calculation of the evaporation constant $K_i$ the value of $Nu_D$ equal to 2 was used in accordance with recommendations in [5, 14, 15].

It can be seen in Fig. 2 that the equilibrium droplet temperature $T_{ki}$. considerably changes during the cycle and using its average value during simulations may result in production of a considerable error in estimating the amount of evaporated fuel during the ignition delay period. During the combustion process at high pressures (more than 100 bar) the value of the equilibrium temperature of droplet corresponding to the critical temperature should be used but in the relatively "cold" characteristic zones such as the dense free spray core and dense core of NWF the temperatures are significantly lower and therefore Eq. (12) should be used for determination of $T_{ki}$..

Table 2. Physical and chemical properties of diesel oil and methanol

| Properties | Diesel oil | Methanol |
|---|---|---|
| Mass fraction of C in the fuel | 0.87 | 0.374 |
| Mass fraction of H in the fuel | 0.126 | 0.125 |
| Mass fraction of O in the fuel | 0.004 | 0.499 |
| Low heating value $H_u$ , MJ/kg | 42.5 | 19.9 |
| Density of fuel at 323 K $\rho_f$ , kg/m$^3$ | 830 | 791.7 |
| Surface tension factor $\sigma_f$ , N/m | 0.028 | 0.022 |
| Dynamic viscosity $\mu_f$ , Pa·s | 0.003 | 0.0006 |
| Enthalpy of evaporation $h_{evap}$ , kJ/kg | 250 | 1173 |
| Liquid fuel heat capacity $C_f$ , J/kg K | 1853 | 2510 |
| Fuel vapor heat capacity $C_{fv}$ , J/kg K | 2223 | 1257 |
| Molar mass of fuel $\mu$, kg/kmol | 190 | 32.04 |
| Diffusion factor $D_{c0}$ at atmospheric conditions, m$^2$/s | 3.7 10$^{-6}$ | 1.5 10$^{-5}$ |
| Temperature $T_1$ , K (Eq. 11) | 480 | 293 |
| Saturated vapor pressure at $T_1$ , MPa | 0.0477 | 0.0276 |
| Critical temperature $T_{cr}$ , K | 710 | 513 |
| Saturated vapor pressure at $T_{cr}$ , MPa | 1.616 | 7.98 |

The calculation of the evaporation rate is carried out by two approaches. The first approach is used for the duration of the ignition delay period in which the evaporated fuel fraction is calculated for every time step using expressions (1) and (2) where $U_{om}$ is a current injection velocity and $d_{32}$ is SMD of the droplets of the Elementary Fuel Mass (EFM) injected during one time step increment in simulations. The rate of the fuel evaporation is calculated separately for every EFM and for every time step a decrease in the diameter of the fuel droplets is defined. Such procedure makes it possible to account for the influence of features in the fuel injection profile on the evaporation intensity and to estimate with a high accuracy the

amount of fuel evaporated during the ignition delay and burnt in accordance with the volumetric mechanism. The second approach covers the diffusion combustion period until the instance when the fuel injection is terminated. At this stage the fuel evaporation rate is calculated using the same Eqs. (1) and (2) but with $U_{om}$ and $d_{32}$ assumed to be equal to the average injection velocity and the average SMD of droplets, respectively (average for whole injection period).
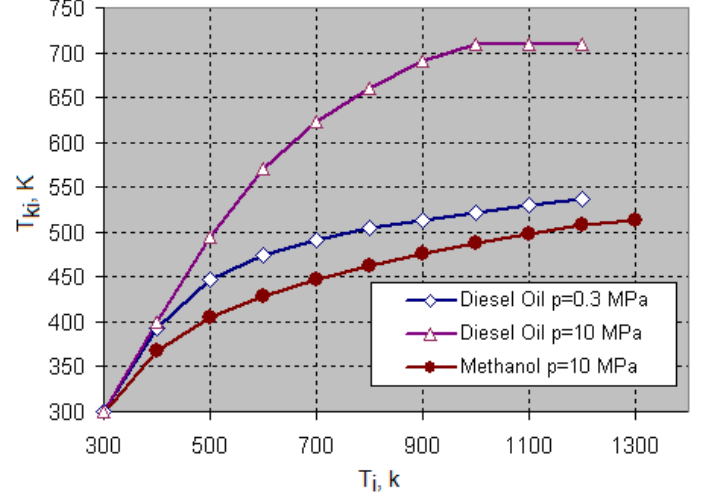


Figure 2. The equilibrium temperature of droplet $T_{ki}$ for diesel oil and methanol as a function of the temperature $T_i$ in the dilute outer characteristic zone of the fuel spray.
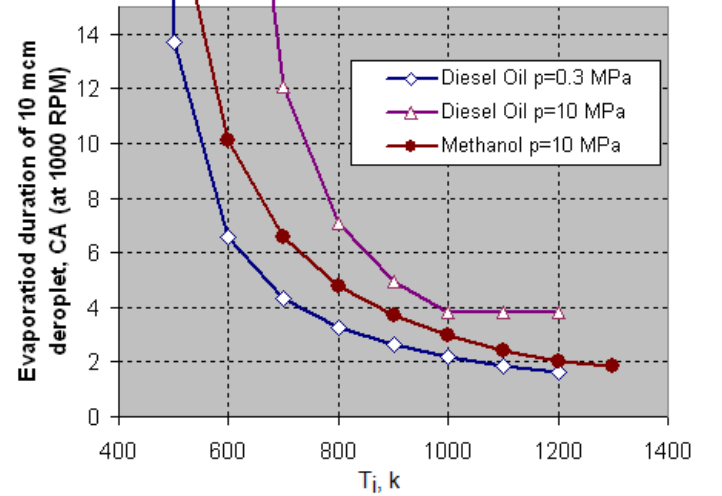


Figure 3. Duration of full evaporation of fuel droplets with the diameter of 10 μm as a function of the temperature $T_i$ in the dilute outer characteristic zone of the fuel spray (in CA deg. for the engine speed of 1000 RPM)

The evaporation rate of fuel in the characteristic zone $i$ is calculated using equation derived analytically by D. N. Vyrubov in [14, 15]:

$$\frac{d\sigma_{ui}}{d\tau} = \left[1 - \left(1 - b_{ui}\,\tau_{ui}\right)^{3/2}\right]\frac{\sigma_{zi}}{\tau_{ui}}\ , \quad b_{ui} = Y\,K_i\big/d_{32}^2\,. \quad (13)$$

4

Here $\sigma_{zi}$ is the current fuel fraction in the characteristic zone $i$, $\tau_{ui}$ is the period of existence of the characteristic zone $i$, $Y$ is the correction factor.

For the late combustion phase (following the termination of the fuel injection) the duration of afterburning is determined by the time $\tau_{i.burn}$ which is necessary for evaporation and combustion of large fuel droplets formed at the end of the injection process [5, 6]. The characteristic diameter of these large droplets $d_l$ is calculated using Eqs. (1) and (2) assuming that $U_{om}$ is the average injection velocity of the last 5% of the fuel injected and $d_l = d_{32}$ is characteristic SMD of the large droplets in the last 5% of EFM's. The time $\tau_{i.burn}$ is calculated as:

$$\tau_{iburn} = d_l^2 / K_u [1 + 2.5 \cdot 10^6 \, K_{ENV} / (\alpha - 1)]$$

where $K_u = Y \, K_{ENV}$; $K_{ENV}$ is the evaporation constant in the dilute outer surrounding of the spray, $\alpha$ is the Air/Fuel equivalence ratio in the cylinder. It is assumed that the large fuel droplets, which were formed at the end of injection with the spray velocity being slow, do not reach the walls and evaporate in the volume after the dense spray core is dissipated.

## CALCULATION OF INGINTION DELAY PERIOD FOR AIR AND METHANOL/N-HEPATNE MIXTURE

The specifics of the methanol ignition significantly differ from those of diesel oil. The Cetane number for methanol is approximately 3 and therefore the typical compression ratio of modern diesel engines is insufficient to ensure the self ignition of this fuel. However, situation radically improves if there is mixture of diesel oil and methanol vapour in the air charge. In this section the analysis of different chemical mechanisms is carried out to describe the oxidation of methanol and n-heptane (which is typically used for estimation of the self-ignition delay period of diesel oil). Corresponding calculations of the ignition delay period were performed using CHEMKIN PRO software.

To determine the period of the ignition delay of the diesel oil a chemical mechanism of the combustion for n-heptane may be deployed. A number of chemical mechanisms were proposed to predict the combustion of n-heptane and in this study the mechanism developed by the Lawrence Livermore National Laboratory (LLNL) [16] is used for simulation of conventional diesel engines. This mechanism includes 1540 chemical reactions between 160 species and may be applied for the arbitrary composition of the air/n-heptane mixture with a residue fraction of combustion products. The mechanism is well tested and results of calculations have shown a good agreement with experimental data. For example, the comparison of simulation and experimental data, obtained for the stoichiometric mixture of n-heptane and air in the shock tube, was presented in [17, 18]

For estimation of the ignition delay period for methanol the Complete San Diego chemical mechanism was described in [19]. The mechanism takes into account 244 chemical reactions

between 50 species and may be applied for the arbitrary composition of air/methanol mixture with a residue fraction of combustion products. Theoretical results obtained using Complete San Diego chemical mechanism were compared to experimental data acquired for the methanol/oxygen/argon blends combustion in shock tubes [20]. Fig. 4 demonstrates a close correlation between theoretical results and experiment for $p = 1.2$ bar and the fuel/air equivalence ratio $\lambda$ of 0.75. In the form presented in [19] the Complete San Diego mechanism cannot be used for a mixture additionally containing n-heptane.

In this study the search was carried out in several stages for the best mechanism to describe combustion of air/n-heptane/methanol blends. Initially, a LLNL air/n-heptane mechanism [16] was tested because it takes into account some of methanol oxidation reactions. However, such approach was not successful and there was a significant deviation between theoretical and experimental results and therefore this mechanism could not be used for modelling the engine fueled by methanol/diesel oil mixture.

At the second stage a combined chemical mechanism of air/n-heptane/methanol combustion was developed which takes into account 1672 reactions between 177 species and brings together Complete San Diego [19] and LLNL [16] mechanisms.

The reaction of methanol with hydrogen dioxide can be described as in [21]:

$$CH_3OH + HO_2 = CH_2OH + H_2O_2 \qquad (14)$$
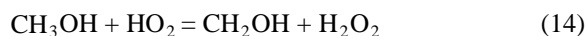
and this reaction has a very strong impact on the methanol ignition delay period. The rates for the forward and back reactions are determined from Arrhenius equation:

$$k_{fi} = A_i T^{\beta_i} \exp\left(\frac{-E_i}{RT}\right), \qquad (15)$$

where $A_i$ and $\beta_I$ are constants for the $i$-reaction; $T$ is the temperature; $E_i$ is the activation energy for the $i$-reaction. Coefficients in the Arrhenius equation for the reaction (14) were obtained from various mechanisms of combustion described in [16, 19, 21] as presented in Table 3. This data was obtained for specific conditions of the methanol/oxygen blend combustion in argon environment at the high temperature and low pressure conditions which considerably differ from those existing in internal combustion engines.

Table 3. Reaction rates parameters

| Forward reaction | | | Reverse reaction | | | Reference |
|---|---|---|---|---|---|---|
| $A$ | $\beta$ | $E$ | $A$ | $\beta$ | $E$ | |
| 3.980e+13 | 0.0 | 19400.10 | 3.130e+15 | -0.9 | 10750.00 | [16] |
| 8.000e+13 | 0.0 | 19383.37 | 8.000e+13 | 0.0 | 19383.37 | [19] |
| 1.00e+12 | | 10047.85 | 2.69e+11 | | -478.47 | [21] |

Additionally, Kumar and Sung determined in [22] reaction rate parameters in Eq. (14) for oxidation of methanol in air at

the pressure level of 29.6 bar and for the temperatures ranging from 880 to 980 K. Such temperature and pressure conditions are closer to that in internal combustion engines. Table 4 presents Arrhenius equation constants proposed in [22] for Eq. (14).

Table 4. Reaction rate parameters by Kumar and Sung [22]

| Forward reaction | | | Reverse reaction | | |
|---|---|---|---|---|---|
| $A$ | $\beta$ | $E$ | $A$ | $\beta$ | $E$ |
| 2.500e+12 | 0.0 | 19400.10 | 6.28e+13 | -0.7 | 11874.3 |

Calculations of the value of the ignition delay period for methanol for conditions in which $p$=1.2 bar and $\lambda$=0.75 were performed using the combined Complete San Diego [19] and LLNL [16] mechanisms with the reaction rate parameters in [19] and though such approach provides an accurate predictions, see Fig. 4, simulation conditions are very different from those in engines.
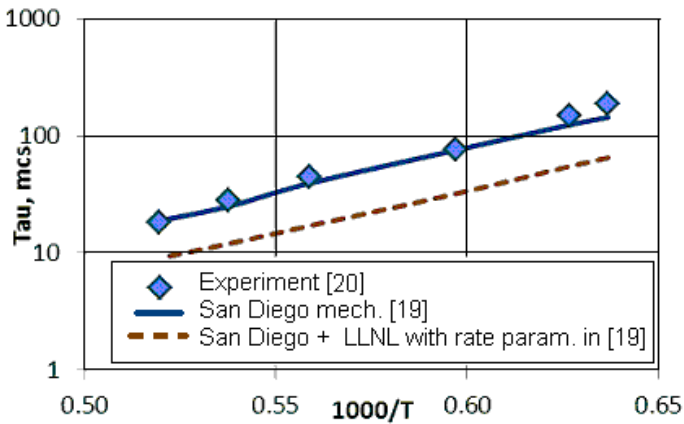


Figure 4. Numerical and experimental data on the value of the ignition delay period for methanol ($p$=1.2 bar, $\lambda$=0.75).

Simulations of the ignition delay period of air/methanol mixture were carried out for $p$=29.6 bar and $\lambda$=1 with the use of coefficients presented in Tables 3 and 4 and the combined Complete San Diego [19] and LLNL [16] mechanism and results were compared with experiments by Kumar and Sung described in [22]. From three sets of data, presented in Table 3, reaction rate parameters in [19] provided closest predictions mechanism (theoretical shown as the red dotted line in Fig. 5). The black line in Fig. 5 presents more accurate predictions obtained with the use of data provided by Kumar and Sung in [22]. However, the precision of predictions shown in Fig. 5 is still not satisfactory for the simulation of the engine's working cycle.

At the third stage the accuracy of theoretical prediction using the Extended LLNL air/n-heptane combustion chemical mechanism was investigated. This mechanism takes into account 2827 reactions between 654 species as described in [23]. The mechanism also accounts for the detailed kinetics in the methanol oxidation. Calculations were performed using reaction rate parameters presented in [22] and [23]. Comparison between calculated and experimental data is presented in Fig. 6 and it can be seen that the extended LLNL mechanism with the reaction rate parameters given in [22] provides a better accuracy in description of the methanol ignition delay (shown as a blue line in Fig. 6).
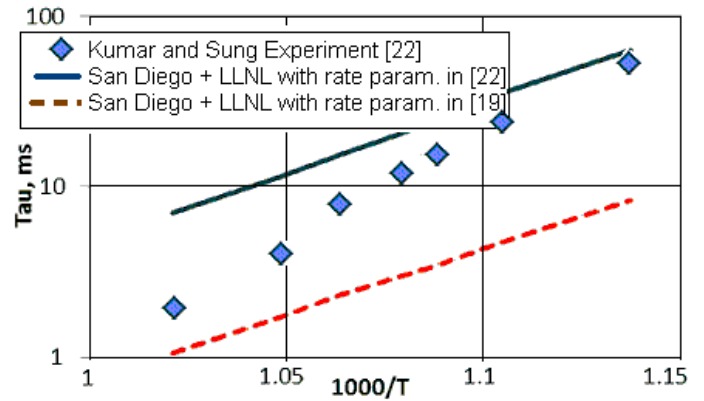


Figure 5. Ignition delay period of air/methanol mixture ($p$=29.6 bar, $\lambda$=1): numerical data was obtained using the combined n-heptane/methanol combustion mechanism which was developed in this study
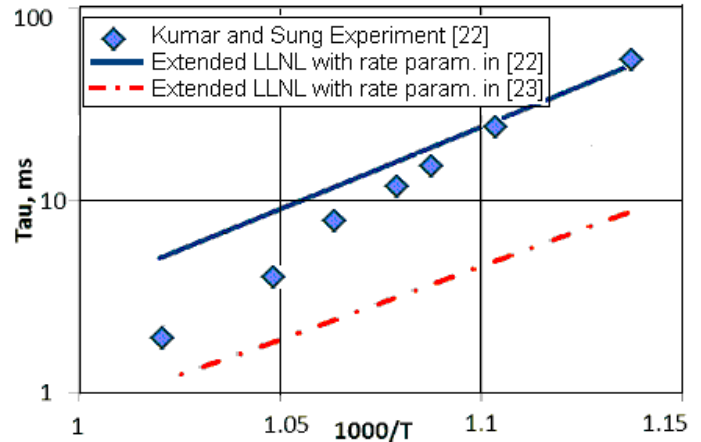


Figure 6. Ignition delay period for air/methanol mixture ($p$=29.6 bar, $\lambda$=1): numerical data was obtained using the extended n-heptane LLNL mechanism of combustion

Therefore the extended LLNL mechanism with the reaction rate parameters given in [22] was selected to carry out further theoretical simulations of engines in this work. In general, there is an opportunity to further improve the accuracy of predictions but this requires more detailed analysis of the mechanism of the methanol oxidation and additionally to take into account kinetic rates of some other key reactions in the mechanism.

There is a very limited published experimental data on estimation of the air/methanol/n-heptane mixture ignition period. Thus, calculations of selfignition of methanol/n-heptane blends with different mass compositions at the pressure value of 40 bar and $\lambda$=1 were performed and the obtained results are presented in Fig. 7. It can be seen that the raise in the methanol content results in the increase of the ignition delay period. The mixture of pure methanol and air doesn't ignite at temperatures below 900 K.

Additionally, calculations were carried out to estimate the ignition delay period for the stoichiometric methanol/air mixture across a wide range of temperatures and pressures.

Calculated results were processed and the following correlation was derived to determine the theoretical ignition delay as a function of the pressure and temperature in the cylinder:

$$\tau_{ign} = 10^{\omega} \ [\text{sec}], \qquad (16)$$

where $\tau_{ign}$ is theoretical ignition delay being function of $p$ & $T$;

$$\omega = a + b \cdot \ln(\Theta) + c \cdot \ln(p) + d \cdot \ln(\Theta)^2 + e \cdot \ln(p)^2 +$$
$$+ f \cdot \ln(\Theta)\ln(p) + g \cdot \ln(\Theta)^3 + h \cdot \ln(p)^3 +$$
$$+ i \cdot \ln(\Theta)\ln(p)^2 + j \cdot \ln(\Theta)^2 \ln(p);$$

$$\Theta = 1000 / T.$$

Here $T$ is the temperature [K], $p$ is the pressure [bar], constants $a$ - $j$ are presented in Table 5.

Eq. (16) is necessary to find the ignition delay period $\tau_i$ using integral of Livengood-Wu:

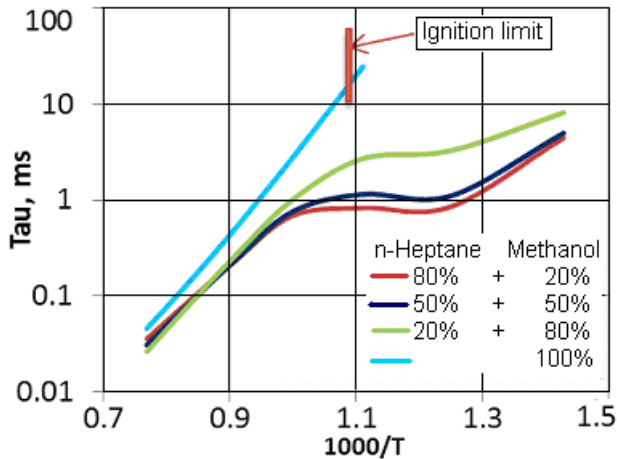$$\int_0^{\tau_i} \frac{d\tau}{\tau_{ign}} = 1 \ . \qquad (17)$$



Figure 7. Ignition delay period for stoichiometric air/n-heptane/methanol blends: numerical data was obtained using the Extended n-heptane LLNL mechanism with the reaction rate parameters suggested in [22] ($p$ = 40 bar)

The accuracy of the correlation in Eq. (16) used for calculation of the ignition delay time in the stoichiometric methanol/air mixture is illustrated in Fig. Annex A. It can be seen that the above correlation provides an acceptable precision with the correlation coefficient value being 0.999. Although Eq. (16) makes it possible to run fast simulations, it does not account for number of important parameters as the composition of the blend of methanol with diesel oil and residual gas effect.

The kinetic mechanisms investigated in this paper do not provide the satisfactory accuracy for a wide range of pressure and temperature conditions in the cylinder with the blend of methanol and diesel oil. Therefore in the current stage of the research the following approach was deployed for determination of the start of ignition: if there is only methanol in the cylinder then Eq. (16) is used for the ignition delay prediction; if there is a mixture of methanol and diesel oil in the engine then the conventional equation for the diesel oil ignition delay period is used as described in [5-12]. In the latter case it is assumed that combustion of methanol starts with the ignition of diesel oil. In the future it is planned to develop an economical method of self-ignitions period prediction using the concept described in [12] enhanced with the capability to take into account the Methanol/Diesel oil ratio in the blend and the effect of the residual gas.

Table 5. Value of constants used in Eq. (16)

| Constants | Value |
|---|---|
| a | -1.13734 |
| b | 7.350526 |
| c | -0.51045 |
| d | 7.268311 |
| e | 4.55e-02 |
| f | 0.408513 |
| g | 0.313734 |
| h | -3.08e-03 |
| i | -3.63e-02 |
| j | -0.30991 |

## REFINING THE SUB-MODEL FOR SIMULATION OF IN-CYLINDER PROCESSES

Methanol evaporates more rapidly than diesel oil and has also the considerably greater enthalpy of evaporation. The enthalpy of evaporation of diesel oil is only 0.58% of its enthalpy of combustion and therefore can be neglected in energy balance calculations. For methanol the ratio of enthalpy of evaporation to heat of combustion is considerably higher and is 5.6%. Therefore these properties of methanol should be taken into account when modelling the in-cylinder processes, especially when the ignition delay period is substantial

compared to the case when only diesel oil is used as fuel. In particular, processes of evaporation and combustion should be distinguished and considered separately during numerical simulations when solving the energy conversation equation. The set of equations for describing the in-cylinder thermodynamic processes includes the following:

$$U_2 - U_1 = -\int_{V_1}^{V_2} p \cdot dV + \sum I_j^* + Q_x - Q_w; \qquad (18)$$

$$m_2 - m_1 = \sum \Delta m_j; \qquad (19)$$

$$p \cdot V = m \cdot R \cdot T, \qquad (20)$$

where $\int_{V_1}^{V_2} p \cdot dV$ is the work done by the working fluid; $I_j^*$ is the enthalpy of the working fluid with the mass of $\Delta m_j$, entering the control system and supplied by the source of mass $j$; $Q_x$ is the heat supplied to the working fluid from the heat source (e.g. combustion); $Q_w$ is the rejected heat; $p, T, m, V, U, R$ are pressure, temperature, mass, volume, internal energy and gas constant of the working fluid. Indices 1 and 2 denote the beginning and the end of the thermodynamic process.

If the engine is equipped with separate $k$ fuel supply systems which are capable to inject different fuels, including that which have the high volatility, then the heat input into the working fluid can be calculated as:

$$Q_x = \sum_{k=1}^{k} \left\{ \left[ \left( \frac{dx}{d\phi} \right)_k \left( H_{u\,k} + h_{evap\,k} \right) - \left( \frac{d\sigma_u}{d\phi} \right)_k h_{evap\,k} \right] \Delta\phi \cdot m_{f\,k} \right\}, (21)$$

where $\left( \frac{dx}{d\phi} \right)_k$ and $\left( \frac{d\sigma_u}{d\phi} \right)_k$ are the heat release rate and the rate of evaporation of fuel injected into the cylinder by the fuel supply system $k$, $\Delta\phi$ is the time step in CA degrees, $m_{fk}$ is the mass of fuel injected into cylinder by the fuel supply system $k$.

The total mass of fuels injected into cylinder at the current time step by all fuel supply systems is:

$$m_F = \sum_{k=1}^{k} \left[ \left( \frac{d\sigma_u}{d\phi} \right)_k \cdot \Delta\phi \cdot m_{f\,k} \right]. \qquad (22)$$

The described modifications in sub-models for calculation of the self-ignition delay period, evaporation and in-cylinder processes are part of the further development made in the core of the mathematical model for simulation of internal combustion engines described in [5-12]. These modifications were realized and additional input interfaces were created in DIESEL-RK software to add the capacity to simulate and optimize dual-fuel engines. In the modified software up to 5 independent fuel injections systems can be specified for an engine, and these can be used for injection of different types of fuel with own injection profiles and sequences. Fig. Annex B shows the interface for data input for two stroke large marine diesel engine with two independent side injectors per cylinder. The interface allows users to deploy several injection systems and each of such systems may have several arbitrary mounted injectors with nozzles having various diameters and arbitrary

orientation. Fig. Annex C shows the Results of sprays behaviour simulation in cylinder of Mitsubishi UEC 45 engine [24] when fuel systems A and B start injection simultaneously. The tool allows analysis of fuel allocation in characteristic zones and optimization of nozzles orientation to minimize spatial contacts of the sprays and their Near Wall Flows (NWF). The volumes of intersected sprays calculated here are used to define fuel mass and equilibrium temperature of evaporated droplets in corresponding zones.

## VALIDATION OF RESULTS OF NUMERICAL MODELLING OF THE WORKING PROCESS OF THE DUAL-FUEL ENGINE

Simulation of the medium speed diesel engine which is equipped with two independent fuel supply systems was carried out and results are presented in this section. Methanol injected by the system B is used as main fuel which is ignited with the pilot injection of diesel oil supplied by the system A, see, Fig. Annex D. This figure demonstrates the Diesel-RK program interface for data input for the dual-fuel engine in which (a) the injector configurations are described; and (b) the fuel injection profiles are specified.

Experimental results for this engine were made available to authors of this paper by the VTT Technical Research Centre of Finland. Diesel oil was injected first in the experiment and methanol was injected then into already burning ambient, so the rate of the pressure rise is not particularly high, namely $dp/d\phi = 3.78$ bar/deg.

Fig. 8 shows dynamics of the heat release during the combustion of diesel oil (supplied by the fuel system A) and methanol (delivered by the fuel system B). The comparison of experimental and computational data shows an acceptable level of accuracy of predictions (for this stage of research). Additionally, Fig. 8 presents information on the heat required for the evaporation of methanol.

The spray tip penetration and the diameter of fuel droplets of diesel oil and methanol are presented in the mid-diagram of Fig. 8. Finally, the bottom diagram of Fig. 8 shows the injection profiles for both fuels.

Fig. 9 demonstrates the result of simulation of diesel fuel spray evolution in the combustion chamber at the end of the diesel oil injection when the injection of methanol into the cylinder only starts. The right diagram in Fig. 9 shows dynamics of the diesel oil distribution in the characteristic zones of the fuel spray and the diesel oil injection profile.

Numerical results of simulation of the methanol spay evolution at the end of its injection are presented in Fig. 10 together with the data on the allocation of methanol in the characteristic zones of the spray.

Finally, Fig. 11 shows a comparison of experimental and theoretical data on the variation of the pressure in the engine's cylinder.

It is planned that further improvements will be made in the near future in the mathematical model to make it possible to account for interactions of sprays of different fuels in the

volume. At this stage the model takes into account only interactions of NWF's of sprays on the surface of the combustion chamber after their impingement on the wall with an arbitrary shape. The latter allows engineers to optimize the piston's bowl shape and orientation of injector nozzles.
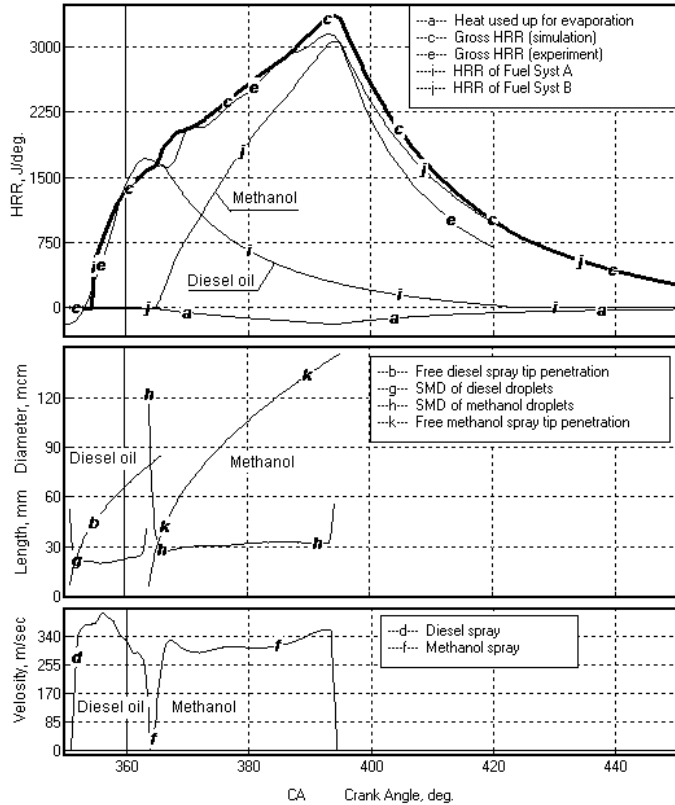


Figure 8. Dynamics of the heat release in combustion of diesel oil (fuel syst. A), methanol (fuel syst. B) and the gross heat release rate from numerical simulations and experimental tests.
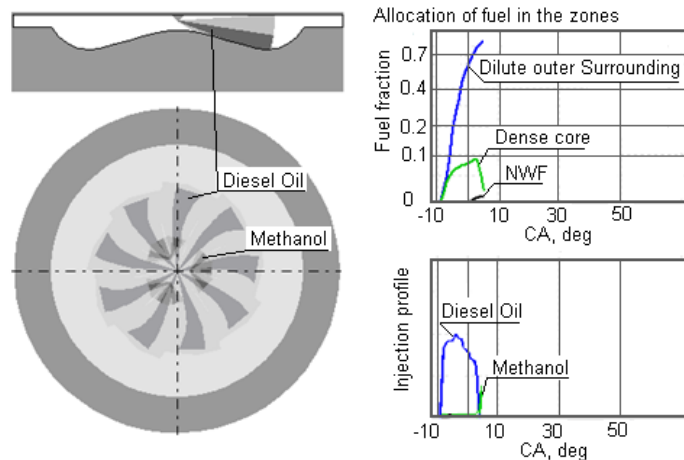


Figure 9. Result of simulation of Diesel oil spray evolution in combustion chamber at the end of Diesel oil injection; the diesel oil distribution in the characteristic zones of the spray.

The zones of the dense conical core of the sprays and near wall flows are shown in dark grey colour.
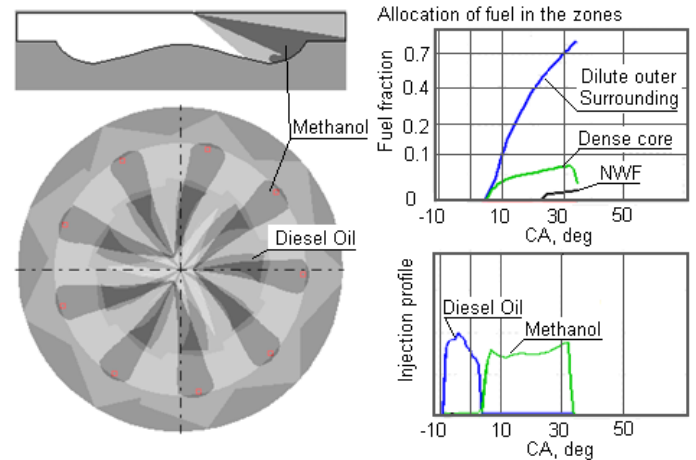


Figure 10. Result of simulation of methanol spray evolution in combustion chamber at the end of methanol injection; the methanol distribution in the characteristic zones of the spray. The zones of the dense conical core of the sprays and near wall flows are shown in dark grey colour.
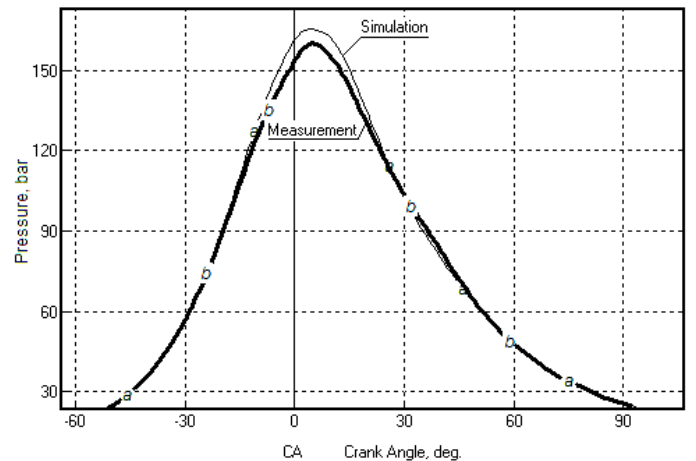


Figure 11. Comparison of theoretical (a) and experimental (b) pressure in the engine cylinder.

## CONCLUSIONS

The existing mathematical model of IC engines was further improved and this makes it possible to simulate the working process of diesel engines equipped with several independent fuel systems for injection of different types of fuel. The modified mathematical sub-models were incorporated into existing thermodynamic DIESEL-RK software and can be used for optimisation of the design of dual-fuel engine and its fuel supply systems.

The obtained theoretical results from simulations of the working process of the medium speed dual-fuel (methanol/diesel oil) engine were compared to experimental

data on the variation of the gross heat release and pressure in the cylinder. Assessment of numerical and experimental results demonstrate that the modified mathematical model provides an acceptable accuracy in prediction of parameters of the working process.

Currently, work is ongoing on the further improvements of the mathematical model described in this paper.

## ACKNOWLEDGMENTS

## ABBREVIATIONS

**C:** Carbon.
**CA**: Crank angle.
**CFD:** Computational Fluid Dynamic.
**CI:** Compression Ignition.
**EFM**: Elementary Fuel Mass injected during one time step increment.
**EGR**: Exhaust Gas Recirculation.
**H:** Hydrogen.
**HRR**: Heat Release Rate.
**IC:** Internal Combustion.
**IMEP:** Indicated Mean Effective Pressure.
**LLNL** : Lawrence Livermore National Laboratory.
**NWF**: Near Wall Flow.
**O:** Oxygen.
**PM:** Particulate matter.
**RON:** Research Octane Number.
**SI:** Spark Ignition.
**SMD:** Sauter mean diameter.

## NOMENCLATURE

*a-j:* Constants.
$A_i$ : Pre-exponential constant for the i-reaction in Arrhenius equation.
$b_m$ : Depth of the spray forward front, m.
$C_f$ : Heat capacity of fuel, J/(kg K).
$C_{fv}$ : Heat capacity of fuel vapour, J/(kg K).
$d_{32}$ : Sauter mean diameter, m.
$D_{co}$ : Coefficient of concentration diffusion at normal conditions, $m^2$/s.
$d_k$ : Current diameter of the droplet, m.
$d_l$ : Characteristic diameter of large droplets, m.
$d_n$ : Nozzle hole diameter, m.
$d_0$ : Initial diameter of the droplet; m.
$D_p$ : Baro-diffusion factor for the fuel vapor under the combustion chamber conditions, s.

$D_{po}$: Baro-diffusion factor of fuel under the atmospheric conditions, s.
$d\sigma_u / d\varphi$: Rate of evaporation of fuel injected into the cylinder, 1/deg.
$d\tau$ : time step, sec.
$dx/d\varphi$: Heat release rate, 1/deg.
$E_i$ : Activation energy for the i-reaction in Arrhenius equation.
$h_{evap}$ : Enthalpy of evaporation of fuel, J/kg.
$H_u$ : Low heating value of fuel, J/kg.
$h_{wfr}$: Height of the forward front of the NWF, m.
$I^*_j$ : Enthalpy of the working fluid with the mass of $\Delta m_j$, J.
$K$ : Evaporation constant.
$K_{ENV}$ : Evaporation constant in the dilute outer surrounding of the spray.
$K_i$ : Theoretical evaporation constant in the *i*-zone.
$M$ : Squared Ohnezorge number.
$m$ : Mass of fluid in the thermodynamic system, kg.
$m_f$ : Cycle fuel mass, kg.
$Nu_D$ : Nusselt number for the diffusion process.
$p_S$ : Pressure of fuel saturated vapor, MPa.
$\rho_f$ : Density of liquid fuel, kg/$m^3$
$p$ : Pressure in the cylinder, MPa.
$p_0$ : Normal pressure: $p_0$ = 0.1 MPa.
$R$ : Gas constant, J/(kg K).
$R_{vap}$ : Specific gas constant of fuel vapour, J/(kg K).
$Q_w$ : Heat loss to the walls from working fluid, J.
$Q_x$ : Heat supplied to the working fluid due to combustion, J.
$T_f$ : Initial temperature of fuel, K.
$T_k$ : Equilibrium temperature of the droplet, K.
$T_0$ : Normal temperature: $T_0$ = 273 K.
$U$ : Internal energy, J.
$U_{om}$ : Velocity of fuel in the nozzle exit, m/s.
$V$ : In-cylinder volume, $m^3$.
$T$ : Temperature, K.
$We$ : Weber number.
$Y$ : Empirical correction function.
$\alpha$ : Air / Fuel equivalence ratio.
$\beta_i$ : Constant for the i-reaction in Arrhenius equation.
$\Delta\phi_j$ : Time step, CA deg.
$\Delta m_j$, : Mass entering into the thermodynamic system from the j-source during time step, kg.
$\varphi$: Crank Angle used at the combustion simulation, deg.
$\lambda$: Fuel / Air equivalence ratio.
$\lambda_a$: Air heat conductivity, W/(m K).
$\mu$ : Molecular mass of fuel, kg/kmol.
$\mu_f$ : Dynamic viscosity of fuel, Pa s.
$\rho$ : Dimensionless density.
$\rho_{air}$ : Air density, kg/$m^3$.
$\rho_f$ : Fuel density, kg/$m^3$.
$\tau$ : Time, sec.
$\tau_i$ : Self ignition delay in conditions of engine cylinder, sec.
$\tau_{t.burn}$ : Time of evaporation and combustion of large fuel droplets formed at the end of the injection, s.

$\tau_{ign}$ : Self ignition delay at the fixed pressure, temperature and composition of mixture, sec.

$\tau_u$ : Current time from the start of evaporation, s.

$\sigma_f$ : Fuel surface stress, N/m$^2$.

$\sigma_u$ : Fraction of fuel evaporated at the current moment of time.

$\sigma_{ui}$ : Fraction of fuel evaporated by the current moment of time in i-zone.

$\sigma_{zi}$ : Current fuel fraction in the characteristic zone *i*.

SUBINDEXES

*1* : corresponds to a low temperature.

*1* : corresponds to beginning of time step.

*2* : corresponds to end of time step.

*air* : Air.

*cr* : Corresponds to critical temperature.

*f* : Fuel.

*i* : i - zone.

*k* : Number of fuel injection system of engine (they are marked in Fig. Annex A as A, B, C, D and E)

## REFERENCES

[1]   http://www.diesel-rk.com (accessed on 2 March.2014).

[2]   Kokjohn, S. L., Hanson, R. M., Splitter, D. A., and Reitz, R. D., 2011, "Fuel reactivity controlled compression ignition (RCCI): a pathway to controlled high-efficiency clean combustion," International Journal of Engine Research, Vol. 12, No. 3, pp. 209-226.

[3]   Toshiyuki, S., 1984, "Methanol diesel engine and its application to a diesel vehicle," SAE Technical Paper 840116.

[4]   Dempsey, A.B., Walker, N.R., Reitz, R., 2013, "Effect of Piston Bowl Geometry on Dual Fuel Reactivity Controlled Compression Ignition (RCCI) in a Light-Duty Engine Operated with Gasoline/Diesel and Methanol/Diesel," SAE Technical Paper 2013-01-0264.

[5]   Razleytsev, N.F., 1980, "Combustion simulation and optimization in diesels", Kharkov: Vischa shkola, 169 p. (In Russian).

[6]   Kuleshov, A.S., 2009, "Multi-Zone DI Diesel Spray Combustion Model for Thermodynamic Simulation of Engine with PCCI and High EGR Level," SAE Technical Paper 2009-01-1956.

[7]   Kuleshov, A.S., 2005, "Model for predicting air-fuel mixing, combustion and emissions in DI diesel engines over whole operating range," SAE Technical Paper 2005-01-2119.

[8]  Kuleshov, A.S., 2006, "Use of Multi-Zone DI Diesel Spray Combustion Model for Simulation and Optimization of Performance and Emissions of Engines with Multiple Injection," SAE Technical Paper N 2006-01-1385.

[9]   Kuleshov, A.S., 2007, "Multi-Zone DI Diesel Spray Combustion Model and its application for Matching the Injector Design with Piston Bowl Shape," SAE Technical Paper 2007-01-1908.

[10]   A.Kuleshov, L.Grekhov, 2013, "Multidimensional Optimization of DI Diesel Engine Process Using Multi-Zone Fuel Spray Combustion Model and Detailed Chemistry NOx Formation Model," SAE Technical Paper 2013-01-0882.

[11]   Kuleshov, A., Mahkamov, K., 2008, "Multi-zone diesel fuel spray combustion model for the simulation of a diesel engine running on biofuel," Proc. Mechanical Engineers, Vol. 222, Part A, Journal of Power and Energy, pp. 309-321.

[12]   A.S. Kuleshov, A.V. Kozlov, K. Mahkamov, 2010, "Self-Ignition delay Prediction in PCCI direct injection diesel engines using multi-zone spray combustion model and detailed chemistry," SAE Technical Paper 2010-01-1960.

[13]   Lyshevsky, A.S., 1971, "Fuel atomization in marine diesels," Leningrad, 248 p. (In Russian).

[14]   Vyrubov, D.N., 1946, "Formation of air/fuel mixture in IC engines. In "Working processes of IC engines", Moscow, MASHGIZ,  pp. 5-54. (In Russian).

[15]   Vyrubov, D.N., 1954, "Method of calculation of fuel evaporation," Publications of BMSTU, Vol. 25, pp. 20-34.

[16]   http://www-pls.llnl.gov/?url=science_and_technology-chemistry-combustion-nc7h16_reduced_mechanism (accessed on 27 March 2014).

[17]   Seiser, H., Pitsch, H., Seshadri, K., Pitz, W.J., and Curran, H. J., 2000, "Extinction and Autoignition of n-Heptane in Counterflow Configuration," Proceedings of the Combustion Institute, Vol. 28, pp. 2029-2037.

[18]   Liang, L., Reitz, R.D., Iyer, C.O., Yi, J., 2007, "Modeling Knock in Spark-Ignition Engines Using a G-equation Combustion Model Incorporating Detailed Chemical Kinetics," SAE Technical Paper 2007-01-0165.

[19]   http://web.eng.ucsd.edu/mae/groups/combustion/ mechanism.html (accessed on 27 March 2014).

[20]   Bowman, C.T., 1975, "A shock-tube investigation of the high-temperature oxidation of methanol," Combustion and Flame, Vol. 25, pp. 343–354.

[21]   Tsuboi, T., Hashimoto, K., 1981, "Shock tube study on homogeneous thermal oxidation of methanol," Combustion and Flame, Vol. 42, pp. 61–76.

[22]   Kumar, K., Sung, C. J., 2011, "Autoignition of Methanol: Experiments and Computations," International Journal of Chemical Kinetics, Vol. 43(4), pp. 175-184.

[23]   http://www-pls.llnl.gov/?url=science_and_technology-chemistry-combustion-n_heptane_version_3 (accessed on 27 March 2014).

[24]   H. Nakagawa, Y. Oda, S. Kato, M. Nakashima, M. Tateishi, 1990, "Fuel Spray Motion in Side Injection Combustion System for Diesel Engines," International Symposium COMODIA 90. pp. 281-286.

## CONTACT INFORMATION

Dr. Sc (Tech), professor Andrey Kuleshov e-mail: andrei.kuleshov@northumbria.ac.uk
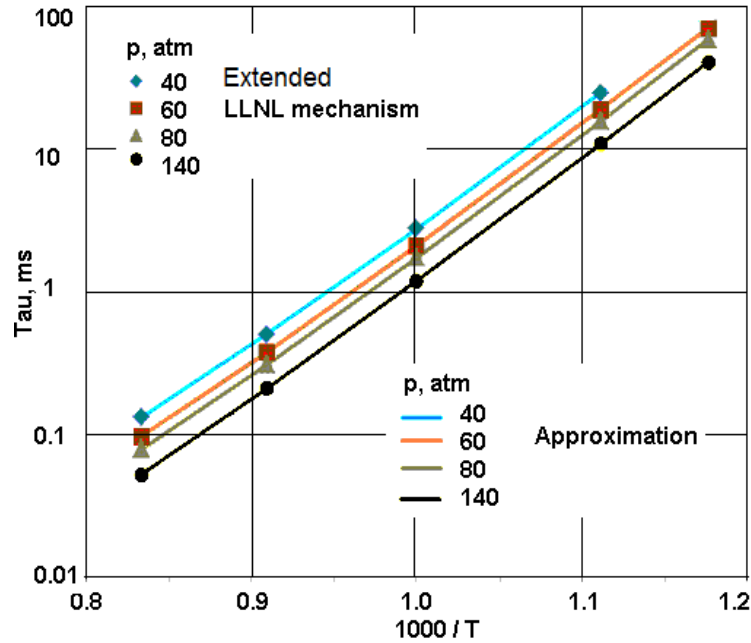
# ANNEX



Figure Annex A.  Accuracy of approximation by Eq. (16): the ignition delay time of the stoichiometric methanol/air mixture calculated using the extended LLNL chemical mechanism with the reaction rate parameters given in [22]
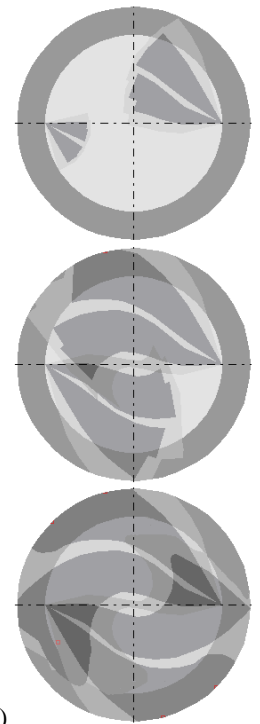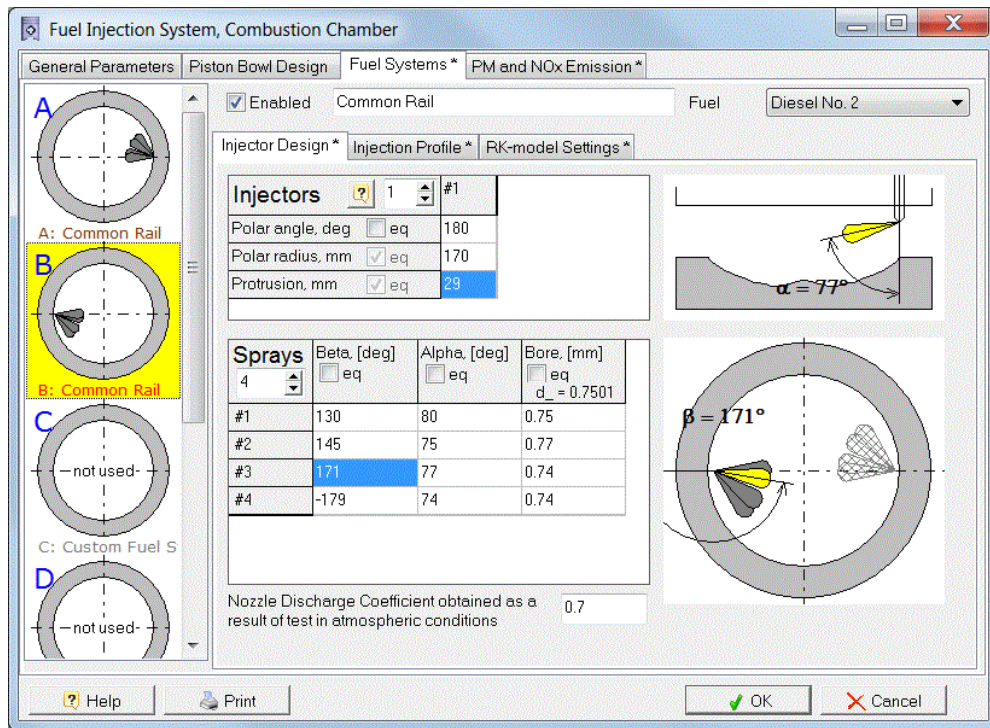


Figure Annex B.  Diesel-RK program interface for data input for the engine with several independently controlled side injectors (a) and results of sprays behaviour simulation in cylinder of Mitsubishi UEC 45 engine [24] at different injection profiles and when fuel system A starts its injection early than fuel system B (b).
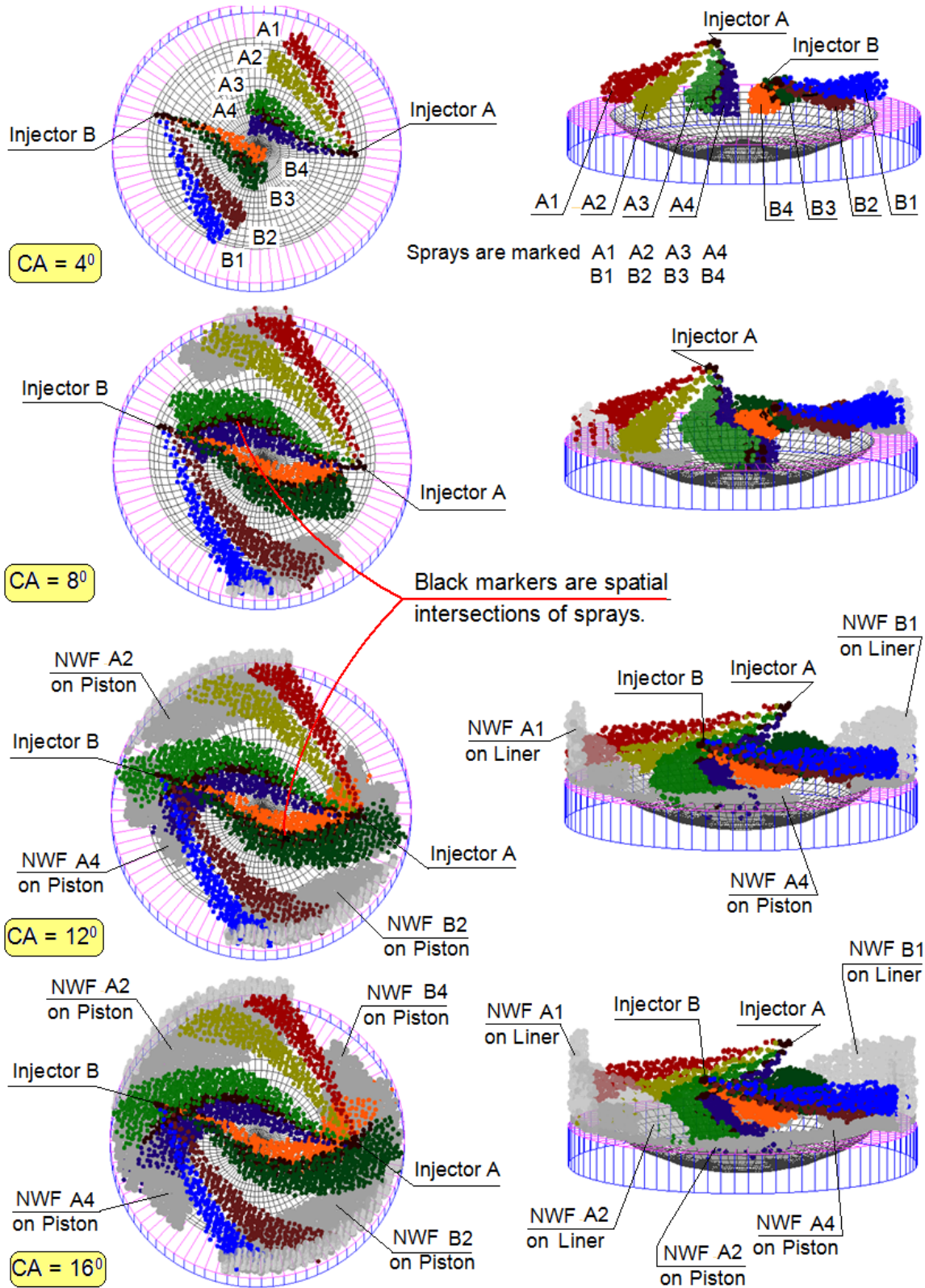
Figure Annex C. Diesel-RK program interface for 3D sprays evolution visualization. Results of sprays behaviour simulation in cylinder of Mitsubishi UEC 45 engine [24] when fuel systems A and B start simultaneously. The tool allows analysis of fuel allocation in characteristic zones and optimization of nozzles orientation to minimize spatial contacts of the sprays and their Near Wall Flows (NWF). Total computational time of full engine cycle (with 3D configuration of 8 sprays) is about 2 min.
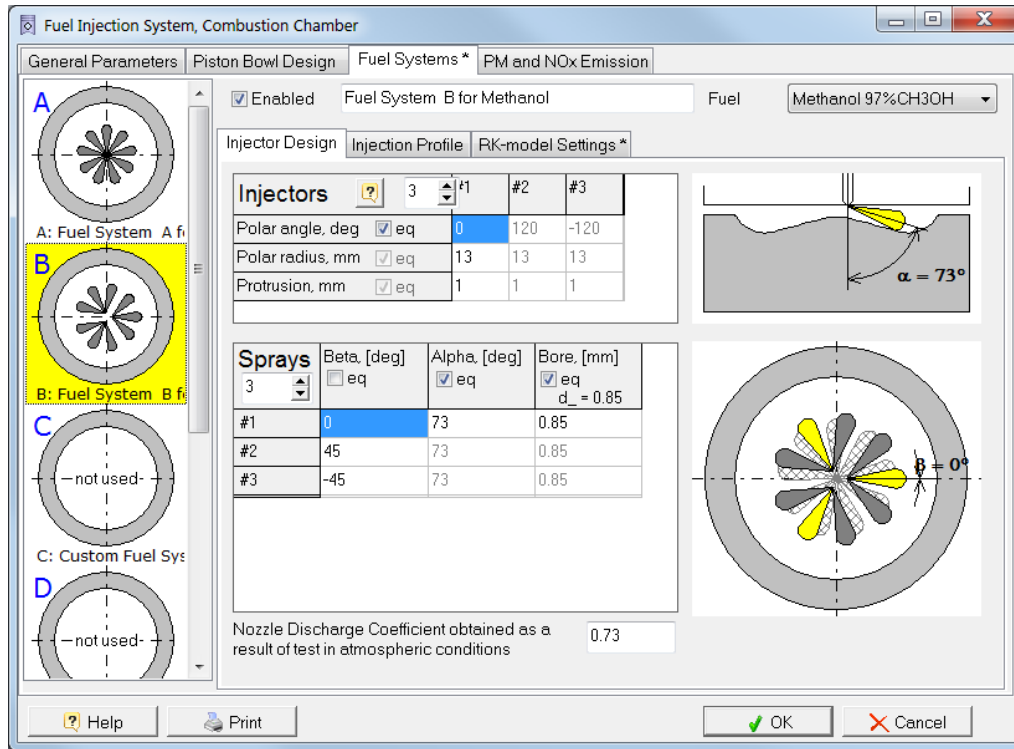
a)
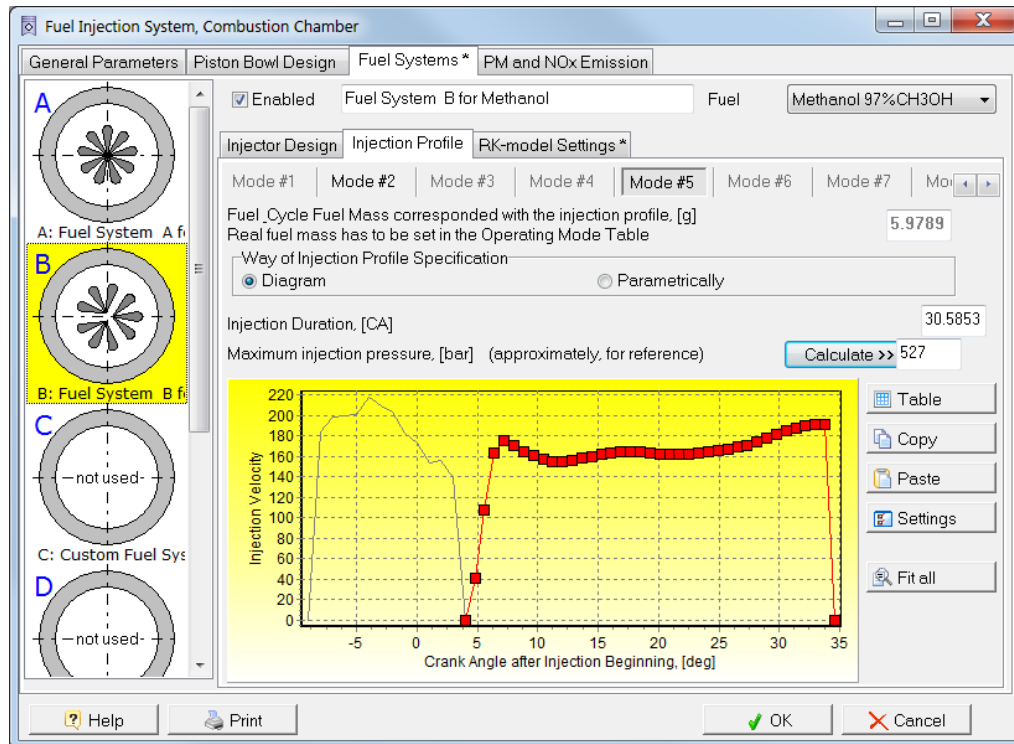


b)

Figure Annex D. Diesel-RK interface for data input for the dual-fuel engine: a) description of the injector configuration; b) description of the fuel injection profiles (data shown is for a medium speed diesel engine which is the object of investigations in this study).